Compact Microstrip Bandpass Filter Improved by DMS and Ring Resonator

Mahdi Oliaei[1, *], Majid Tayarani[2], and Mahmood Karami[1]

Abstract—In this paper, complementary split ring resonators (CSRRs) as band-stop elements are used in combination with coupled microstrip lines as high and low pass elements to design and fabricate very compact bandpass filter (BPF) having controllable characteristics. The proposed filter provides several advantages such as compactness (occupying area less than $0.1\lambda_g \times 0.1\lambda_g$ in which λ_g is calculated at center frequency of pass band), sharp rejection, suitable insertion loss (IL 3-dB bandwidth of roughly 2 GHz from 0.7 GHz to 2.7 GHz, i.e., more than 115% FBW), good return loss (RL less than -8.5 dB in all of the bandwidth) and low cost. Defected Microstrip and Ring Resonator Structures have been used for eliminating the created spurious pass band in upper frequencies. The simulation results have been done with full-wave softwares, i.e., CST MWS and ANSYS HFSS by time and frequency domain solvers, respectively. Also, the equivalent lossless lumped circuit of total structure has been obtained and simulated by ADS software. These simulated results show good agreements with experimental ones.

1. INTRODUCTION

Progressing application of microwave systems in wireless communication defines new trend of microwave technology going toward attaining smaller dimensions everyday in addition to high performance. The use of artificial materials (i.e., not present in nature) with special electromagnetic properties is considered as a very promising technique to obtain small size filters. The behavior of these materials was first characterized by Veselago [1]. They consist of a media with simultaneous negative electric permittivity and magnetic permeability. These materials are known as left handed materials (LHM), since the pointing vector S and the wave vector k are in anti-parallel. These materials consist of resonant elements such as well-known split ring resonators (SRRs) and complementary split ring resonators (CSRRs). In [2], a microstrip combline bandpass filter (BPF) with a broad upper stopband performance was presented. This filter was based on the design of a passband filter cascaded with a defected microstrip structure (DMS) bandstop filter. In [3], a novel ultra-wideband (UWB) bandpass filter (BPF) with improved upper stopband performance using a defected ground structure (DGS) was presented in this letter. In [4], a low IL, sharp rejection wideband microstrip BPF with 3-dB fractional bandwidth of (FBW) 49.3% was designed using stub tuned dual mode ring resonators. But, this filter had undesired pass bands in both sides of the main pass band. In [5], the parallel coupled microstrip line with ground plane aperture technique was proposed to design a compact multipole BPF having 60% FBW with gradual cutoff. In [6], complementary split ring resonators (CSRRs) are proposed to design compact BPFs having wide FBW variation. Here in this paper, recent configurations are improved using new structures such as defected microstrip structure (DMS) [7–10] and full and/or half wave ring resonators as transmission zeros to improve reject and spurious response. CSRR provides a negative effective permittivity in the proximity of its resonant frequency and produces sharp rejection stop band. The proposed approach is suitable for lower as well as higher FBW filters without employing any grounded via.

* Corresponding author: Mahdi Oliaei (m.oliaei90@ee.kntu.ac.ir).
[1] Electrical & Computer Engineering Department, Khaje Nasir Toosi University of Technology (KNTU), Tehran, Iran. [2] Electrical & Electronic Engineering Department, Iran University of Science and Technology (IUST), Tehran, Iran.

2. THEORY

The band pass filter is made of two general parts: the low-pass and high-pass sections. The combination of these two parts form the band-pass filter. The prime structure is mentioned in [6]. In high-pass section, microstrip structure on the top layer is bended in S shape for compactness. In the bottom layer, the metamaterial structure (CSRR) is inserted for controlling the resonant frequencies. The gap provides a negative permeability, and a left handed (LH) transmission band is created. The lower transmission band is LH while the upper one is right handed (RH). A wide passband can be obtained by overlapping the LH and RH bands. High pass filter (HPF) cutoff frequency is mainly determined by the CSRR dimensions.

HPF section can be modeled by an equivalent circuit as shown in [6]. Increased C_g (gap capacitance for HPF section) shifts the RH band towards lower frequency, whereas, increased C_c (Coupling capacitance between top and bottom layers) decreases HPF cutoff frequency, and wider LH transmission band is obtained. At optimized C_g and C_c, LH and RH bands overlap. L_r and C_r are the elements of CSRR which determine the resonant frequency (Fig. 2). In LPF section, two shunt stubs which are formed in U-shape have been used for determining the upper cutoff frequency of the filter. In the bottom layer of this section, a CSRR has been inserted in order to control the second resonant frequency due to LPF with sharp transition knee. The coupling factor between CSRRs and upper lines can be controlled by C_c, and the cutoff frequency of the resulting LPF can be changed as a result. Using the equivalent circuit of a transmission line with CSRR (Fig. 2), the lower frequency of resonance for this
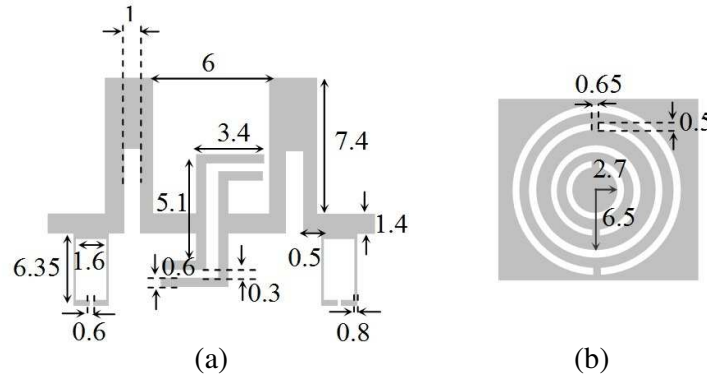
Figure 1. The optimized structure distributed model: (a) top layer, (b) bottom layer.
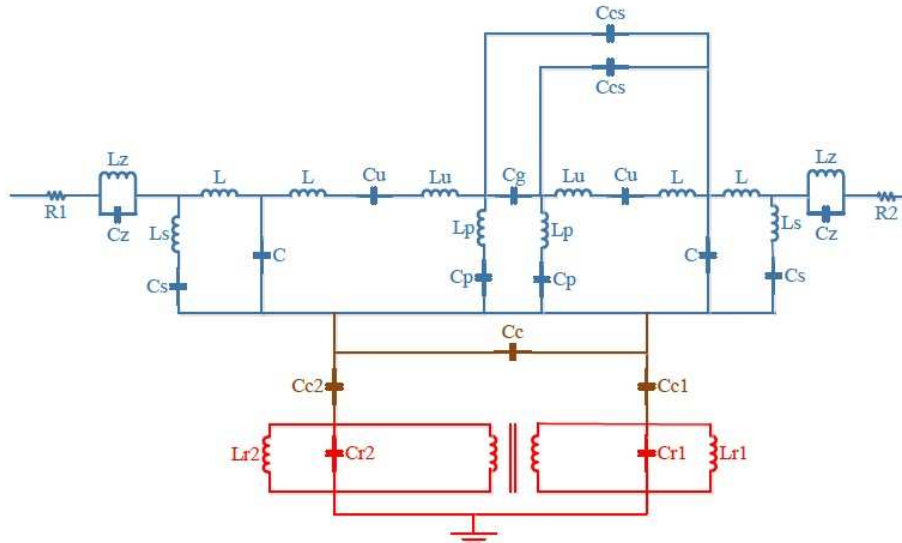
Figure 2. Equivalent lossless lumped circuit for the optimized structure.

circuit is obtained as [11]:

$$f_L = \frac{1}{2\pi\sqrt{L_r\left(C_r + \frac{4}{\frac{1}{C_g} + \frac{4}{C_c}}\right)}} \tag{1}$$

If series impedance of equivalent circuit is dominated by C_r (without considering L), higher frequency of resonance is calculated easily as:

$$f_H = \frac{1}{2\pi\sqrt{L_r C_r}} \tag{2}$$

And the transmission zero for this resonant can be attained by:

$$f_z = \frac{1}{2\pi\sqrt{L_r(C_r + C_c)}} \tag{3}$$

If $C_c \ll 4C_g$, f_z is so close to f_L, and the structure has a very sharp cutoff on lower edge of LH passband. The main structure (BPF) includes these LPF and HPF cascaded. In other words, the lower cutoff frequency of this BPF is determined by the cutoff frequency of the HPF section and the upper one by the LPF section. Of course, the cutoff frequencies can be varied by changing respective dimensions. The proposed compact structure using the defected microstrip structure (DMS) and ring resonators (RRs) which is constructed of two explained sections is shown in Fig. 1.

3. CIRCUIT MODEL

Finally, we have an equivalent circuit similar to that described in [12], which is able to obey the resonant condition to close the stopbands and to ensure CRLH operation in two frequency bands. Due to the frequency dependence of all equivalent circuit elements used in this structure, a complex optimization process of both distributed and lumped circuits is performed in design procedure with the CST Microwave Studio (CST MWS), ANSYS HFSS and Advanced Design System (ADS) softwares. The equivalent lumped circuit for distributed improved structure is shown in Fig. 2. The discontinuities between characteristic impedances of transmission lines on the top layer are replaced by their π or T equivalent circuits [12]. By moving the two CSRRs shown in [6] and allocate them concentrically to achieve a compact structure such as shown in Fig. 1, the coupling effect between two CSRRs includes both electric and magnetic couplings. The effect of electric coupling between these CSRRs can be shown by C_c element, and magnetic coupling is proposed to model by a $1:1$ transformer approximately. The lumped-element values are illustrated in Table 1.

Table 1. Element values of optimized lossless lumped circuit with substrate type of Rogers RO4003, substrate constant of $\epsilon_r = 3.55$, substrate thickness $= 0.508\,\text{mm}$, and metalization thickness $= 0.018\,\text{mm}$.

Parameters	C_g	C_{cs}	L_z	C_z	L
Values	4.3 fF	0.2 fF	0.03 nH	33 pF	0.21 nH
Parameters	C	L_s	C_s	L_p	C_p
Values	0.5 pF	2 nH	2.4 pF	6 nH	0.9 pF
Parameters	L_u	C_u	C_{cs}	C_{c1}	C_{c2}
Values	0.18 nH	0.18 pF	0.2 pF	17 pF	17 pF
Parameters	C_c	C_{r1}	L_{r1}	C_{r2}	L_{r2}
Values	12 pF	1.5 pF	11 nH	1 pF	5 nH

4. SIMULATION RESULTS

The scattering parameters (S) diagram of improved structure is illustrated in Fig. 3. Without exploiting the DMS Ring Resonators, S_{11} and S_{12} parameters are not good at all. Small discontinuous in center

frequency of passband and upper cutoff frequency, existing spurious band in upper side of passband are the disadvantages of this structure. The return loss in the best case is approximately $-17.5\,\text{dB}$, which is not enough, i.e., the resonances are not suitable. Because of these flaws, an improved structure by using defected microstrip structure (DMS) and half-wave Ring Resonators (RRs), as shown in Fig. 1, is introduced. Simulation results are illustrated in Fig. 3. In this case, the resonance frequencies are suitable and S_{11} and S_{12} parameters improved. The transmission frequency is roughly $1.7\,\text{GHz}$. In HP section (below this frequency) for series and parallel resonances, the capacitance and inductance properties are dominant, respectively. On the other hand, in LP section (above of transmission frequency) for series and parallel resonances, the inductance and capacitance properties are dominant, respectively. Therefore, the equivalent circuits can be simplified in HP and LP sections respectively.
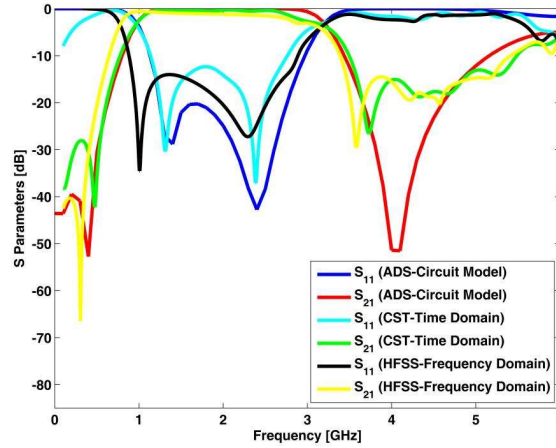
Figure 3. Comparison between different methods of simulation.

As shown in Fig. 3, the 3-dB simulated bandpass frequency starts at $0.7\,\text{GHz}$ and terminates in $2.7\,\text{GHz}$. Therefore, the total 3-dB transmission bandwidth of the filter is $2\,\text{GHz}$. Also, the $-10\,\text{dB}$ bandwidth of S_{11} parameter is $1.6\,\text{GHz}$, which starts from $1.1\,\text{GHz}$ to $2.7\,\text{GHz}$ (the applicable band). Note that the determined filter's parameters indicate its worldwide ISM (Industrial, Scientific and Medical) band applications, which have been allocated by the Federal Communication Commission (FCC), such as GSM900/1800 for cellphones, wireless LANs and cordless phones in $915\,\text{MHz}$ and $2.45\,\text{GHz}$ bands like bluetooth and WiFi devices, etc. The rejection level of lower and upper bands of this filter is average $110\,\frac{\text{dB}}{\text{GHz}}$ and $50\,\frac{\text{dB}}{\text{GHz}}$, respectively. The fabrication parameters of these results shown in Fig. 6 are the same as the simulation results shown in Fig. 3.

5. EXPERIMENTAL RESULTS

A typical sample of compact fabricated improved filter is shown in Fig. 4.
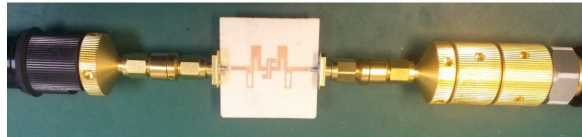
Figure 4. A sample of fabricated improved filter.

Figure 5 shows the measurement process of fabricated filter by ENA Series Network Analyzer.

As shown in Fig. 6, the experimental result and one of the simulation results (ANSYS HFSS) are in good agreement. Consequently, this verification indicates the correctness of simulation results in Fig. 3 for distributed and lumped circuits.
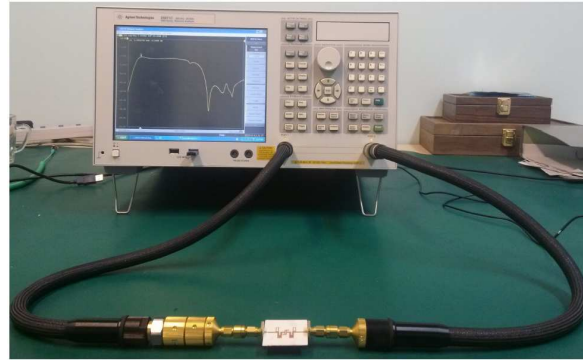
Figure 5. Fabricated filter measurement by network analyzer.
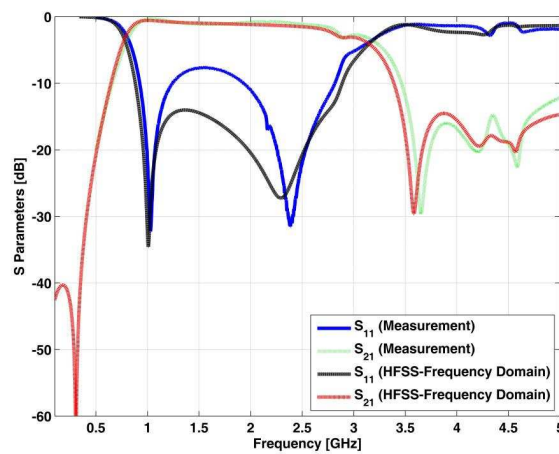
Figure 6. Comparison between simulation and measurement results.

Table 2. Elliptic filter (minimum degree required for designed and fabricated filter parameters achievement).

Parameters	N Degree of Filter	f_0 (GHz)
Values	5	2
Parameters	BW (GHz)	Pass-band Ripple (dB)
Values	2.3	1
Parameters	Attenuation at Stop-band Edges (dB)	Maximum Rejection Level (dB)
Values	40	50

The frequency response of the improved structure shows that we can model it by an elliptic standard filter with characteristics mentioned in Table 2. The minimal values of the proposed elliptic filter required for the designed and fabricated filter parameters have been presented in this table.

6. CONCLUSION

We have discussed filters using metamaterials and investigated their effects on improving frequency response of the structures. Complementary split ring resonators (CSRRs) as band stop elements were used in combination with coupled microstrip lines as high and low pass elements to design and fabrication very compact bandpass filter (BPF) having controllable characteristics. The final filter provided several

advantages such as compactness (occupying area less than $0.1\lambda_g \times 0.1\lambda_g$ where λ_g was calculated at the center frequency of pass band), sharp rejection, suitable insertion loss (IL 3-dB bandwidth of roughly 2 GHz from 0.7 GHz to 2.7 GHz, i.e., more than 115% FBW), good return loss (RL less than -8.5 dB in all of the bandwidth) and low cost. Defected microstrip and ring resonator structures are used for eliminating the created spurious pass band in upper frequencies. The simulation results were obtained full-wave softwares, i.e., CST MWS and ANSYS HFSS by time and frequency domain solvers, respectively. Also, the equivalent lossless lumped circuit of total structure was obtained and simulated by ADS software. These simulated results presented good agreements with experimental ones. Overall, this compact filter can be effectively used for microwave and RF frequencies.

ACKNOWLEDGMENT

REFERENCES

1. Veselago, V. G., "The electrodynamics of substances with simultaneously negative values of ϵ and μ," *Sov. Phys. Usp.*, Vol. 10, 509–514, 1968.
2. Almalkawi, M. J. and V. K. Devabhaktuni, "Compact realization of combline bandpass filter integrated with defected microstrip structure bandstop filter," *Progress In Electromagnetics Research Letters*, Vol. 35, 99–105, 2012.
3. Lee, J. and Y. Kim, "Ultra-wideband bandpass filter with improved upper stopband performance using defected ground structure," *IEEE Microw. Wireless Compon. Lett.*, Vol. 20, No. 6, 316–318, Jun. 2010.
4. Hsieh, L. H. and K. Chang, "Compact, low insertion-loss, sharp-rejection, and wide-band microstrip bandpass filters," *IEEE Trans. Microw. Theory Tech.*, Vol. 12, No. 4, 1241–1246, 2003.
5. Zhu, L., H. Bu, and K. Wu, "Broadband and compact multi-pole microstrip bandpass filters using ground plane aperture technique," *Proc. Inst. Elect. Eng.*, Vol. l49, No. 1, 71–77, 2002.
6. Mondal, P., M. K. Mandal, and A. Chaktabarty, "Compact bandpass filters with wide controllable fractional bandwidth," *IEEE Microwave and Wireless Components Letters*, Vol. 16, No. 10, 71–77, 2006.
7. Fallahzadeh, S. and M. Tayarani, "A compact microstrip bandstop filter," *Progress In Electromagnetics Research Letters*, Vol. 11, 167–172, 2009.
8. Fallahzadeh, S., H. Bahrami, A. Akbarzadeh, and M. Tayarani, "High-isolation dual-frequency operation patch antenna using spiral defected microstrip structure," *IEEE Antennas and Wireless Propagation Letters*, Vol. 9, 122–124, 2010.
9. Mallahzadeh, A. R., B. Rahmati, M. Alamolhoda, R. Sharifzadeh, and A. H. Ghasemi, "Ultra wide stop band LPF with using defected microstrip structures," *IEEE Conference Publications, 6th European Conference on Antennas and Propagation (EUCAP)*, 1–3, 2012.
10. Liu, H. W., Z. C. Zhang, S. Wang, L. Zhu, X. H. Guan, J. S. Lim, and D. Ahn, "Compact dual-band bandpass filter using defected microstrip structure for GPS and WLAN applications," *IET Journals & Magazines, Electronics Letters*, Vol. 46, 1444–1445, 2010.
11. Marques, R., F. Martin, and M. Sorolla, *Metamaterials with Negative Parameters, Theory, Design, and Microwave Application*, John Wiley & Sons, Inc., 2008.
12. Hong, J. S. and M. J. Lancaster, *Microstrip Filters for RF/Microwave Applications*, John Wiley & Sons, Inc., 2001.